

Quadrupedal trotting with active compliance

Ioannis Havoutis Claudio Semini Jonas Buchli Darwin G. Caldwell

Abstract— We present a trotting controller for a torque controlled quadruped robot. Our approach uses active compliance to overcome difficulties that are crucial for the realisation of symmetric gaits, i.e. force equalization, disturbance rejection and impact absorption. We present a scheme for the compliant control of each leg that is based on a *virtual spring* abstraction. This active compliance scheme allows us to greatly vary the dynamical behaviour of the system on-the-fly, without altering the physical characteristics of the robot, by changing the parameters of the virtual springs. This way we are able to evaluate a wide range of trotting gaits with varying parametrizations. We report results of robust trotting in various speeds and push recovery in simulation, and continue with results of actively compliant trotting on the real quadruped robot. We further discuss difficulties and limitations with the implementation of such dynamic gait controllers on the real system.

I. INTRODUCTION

Legged robots can provide superior locomotion characteristics in terms of agility and versatility. Legged platforms can perform both in unstructured environments, where only a number of discrete footholds might be possible (disaster sites, construction sites, forests, etc.), and in situations of smooth, continuous support (flats, fields, roads, etc.). Reaching the potential agility and efficiency, e.g. as observed in quadruped animals, on real robotic platforms has proven to be a major challenge for the robotics community.

In this paper we present a controller that realises a trotting gait on the hydraulically actuated quadruped HyQ [1] (Fig. 1). Our controller is capable of trotting at varying speeds, turning and recovering from pushes. It utilizes active compliance, built on a high-bandwidth force control loop over hydraulic actuators, that is controlled to behave as a virtual spring abstraction. Overall we use simple control loops for the dynamic behaviour of the robot, following the insights of symmetry-based controllers [2] and the *spring-loaded inverted pendulum* (SLIP) paradigm [3]. Such simple feedback loops have been shown to work with *very compliant telescopic* legs in the past [2]. These approaches have been known to work in theory for simplified models but are notoriously hard to implement on real robotic quadrupeds with articulated legs and considerable size. To our knowledge, we are the first to report results of such controllers on a fully actuated quadruped with articulated legs and no physical compliant elements. We show that the utilization of our active compliance scheme makes possible the successful



Fig. 1. The hydraulically actuated quadruped robot - HyQ. It has 12 degrees of freedom and its size is comparable to a goat. HyQ is designed for highly dynamic behaviour, e.g. trotting and jumping.

implementation of simple control laws, that build up a trotting controller for the real quadruped robot.

II. RELATED WORK

A sizeable body of literature has been devoted to modelling the various aspects of quadrupedal locomotion in nature, typically based on the SLIP model. Heglund and Taylor [4] presented a study of quadrupedal locomotion ranging from mice to horses, analysing the relationship between speed, stride frequency and the relationship to different body sizes and gaits. Farley et al. [5] in another large scale biological study estimated from observed data the relationship between speed and animal size with the spring stiffness that the SLIP model predicts, and how this is reflected to the individual legs of the animals. Lee and Biewener [6] have presented a study on the cost of transport, the leg compliance and the leg geometry to inform the design of a large-dog sized quadrupedal robot, Boston Dynamics' *BigDog*.

Poulakakis et al. [7] investigated the passive dynamics of bounding and pronking gaits on the quadruped robot *SCOUT II*. This robot has single-DoF passive-spring legs, while a sagittal plane model has been used for studying the behaviour of the controllers as it lends naturally to such gaits. This way they were able to numerically compute return maps that generate a passively stable behaviour. Estremera and Waldron [8] presented a control algorithm based on leg thrust control for the stabilization of pronking and bounding on the *KOLT* quadruped robot, mostly in simulation and partially on the real robot. Hawker and Buehler [9] experimented with trotting with a quadrupedal robot, a different version of the *SCOUT II* robot mentioned earlier, with legs that have a passive-knee joint combined with a locking mechanism for the stance phase. They presented results of trotting with the

I. Havoutis, C. Semini and D.G. Caldwell are with the Department of Advanced Robotics, Istituto Italiano di Tecnologia (IIT).
<ioannis.havoutis>, <claudio.semini>, <darwin.caldwell>@iit.it.

J. Buchli is with the Agile & Dexterous Robotics Lab, ETH Zurich.
buchlij@ethz.ch

robot on a treadmill mounted on a device that eliminated the need for control of the robot’s roll orientation. Yamada et al. [10] evaluated a bio-inspired approach on a pneumatic muscle driven quadruped robot. Recently, Kotaka et al. [11] reported preliminary in-place trotting experiments on a small-size electrically actuated quadruped.

The seminal work of Raibert [2] has been very influential on the quadruped locomotion community. He has shown how single leg hopping controllers can be ported to bipedal and quadrupedal robots, using a set of sub-controllers that are coordinated by an event-driven state machine. The trotting controller presented in this paper borrows much from Raibert’s work and demonstrates how similarly simple control laws can be implemented on a large scale quadruped robot without passively compliant elements, such as real springs and/or dampers. Last, Boston Dynamics’ *BigDog* has been the most successful field quadruped robot to date. The stability and robustness of *BigDog* has been demonstrated through various media outlets, alas, no experimental data concerning the mechanical design or control of the robot has been published to date.

III. THE TROT

Legged animals employ a multitude of gaits to successfully locomote through varying terrains, ranging from slow walking to fast running gaits. As observed in nature [12], different gaits are more suitable for different locomotion speeds, while gait transitions also depend on the physical characteristics of the systems in question [4], [13]. Gait preference is affected by given locomotion requirements (short sprint, long run, walk) and the dynamical properties of the system (mass, springs/tendons, muscle/motor capabilities), leading to locally optimal solutions with respect to stability, speed, energy expenditure, etc. [4], [14].

The trot is a symmetrical gait in which diagonally opposite legs swing in unison. This provides significant stability advantages while the legs work together to propel the animal/robot and to cushion impact forces. Most mammals use the trot when running and a considerable subset of quadrupeds have no other symmetrical running gait [12].

The trot has been one of the most common gaits also with quadruped robots. There are a number of reasons for this preference. As mentioned earlier the legs working in unison allow for a better division of the total force that the leg actuators should be able to provide, when receiving impact forces, when supporting the weight of the robot and when thrusting the robot into a flight phase. In addition, during the trot the center of gravity (GoG) of the system is on average kept above or very close to the *line of support* that the stance legs define. This leads to a more stable gait with respect to the robot’s attitude, in contrast to bounding and pronking. Also trotting can cover a large range of velocities, with slow walking trots of very short -or no- flight phase to fast trotting with large flight phases. In addition, the trot being a symmetrical gait, allows for easy anchoring of single leg control templates to the full quadrupedal system [2].

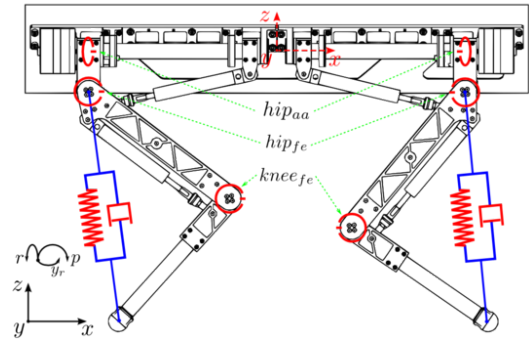


Fig. 2. Mechanical drawing of HyQ with the virtual linear spring and damper model overlaid. Each leg has 3 torque-controlled joints which in order from body to foot are the hip abduction-adduction joint (hip_{aa}), the hip flexion-extension joint (hip_{fe}), and the knee flexion-extension joint ($knee_{fe}$).

IV. HYQ QUADRUPED

Our platform, HyQ (Fig. 1), is a fully torque-controlled hydraulically and electrically actuated quadruped robot comparable in size to a goat ($\sim 70kg$), e.g. an *Alpine ibex*. It has been designed and built *in-house* and it uses a combination of hydraulic cylinders and electric motors for the actuation of its 12 joints [15]. HyQ is capable of highly dynamic locomotion as hydraulic actuation allows the handling of large impact forces, high bandwidth control, high power-to-weight ratio and superior robustness.

Each leg has three degrees of freedom (*DoFs*), two in the hip (abduction/adduction (hip_{aa}) and flexion/extension (hip_{fe})) and one in the knee (flexion/extension ($knee_{fe}$)) (Fig. 2). The hip_{aa} joints are actuated by electric motors while all the hip_{fe} and the $knee_{fe}$ joints are hydraulically actuated. All of the quadruped’s joints are equipped with high resolution encoders and load cells, that allow a smooth control of both position and torque [16], [17]. Overall the robot weighs $70kg$, it is $1m$ long and $0.5m$ wide and stands $1m$ high with the legs fully stretched. The system is controlled by a Pentium PC104 running real-time Linux (*Xenomai*) and is capable of reaching a $1kHz$ control frequency.

V. APPROACH

We combine a traditional pairwise-symmetric trotting controller with a virtual-spring abstraction for each leg. This active compliance scheme allows us to greatly vary the dynamical behaviour of the system on-the-fly, without altering the physical characteristics of the robot (e.g. changing physical springs in the robot legs), by changing the parameters of the virtual springs, i.e. the stiffness, damping and rest length. This way we are able to evaluate a wide range of trotting gaits with varying parametrizations. In addition, it simplifies the control of each leg, as the controller can regard each articulated leg as a virtual telescopic leg. The following two subsections describe the virtual spring abstraction and the controller design.

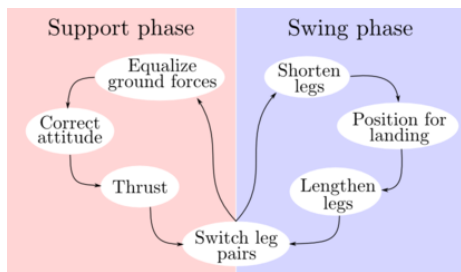


Fig. 3. Schematic diagram of the state machine used for the coordination of the different controller tasks. On the left are the tasks that the support leg pair is concerned with, while on the right are the tasks that concern the swing legs. Note that support and swing phases are concurrent but refer to the diagonally symmetric leg pairs.

A. Virtual components

To achieve active compliance we implemented a virtual linear spring and damper model that is anchored for each leg, on one end at the corresponding hip_{fe} joint and on the other end at the foot, as shown in Fig. 2. To mimic the dynamic behaviour of the virtual spring we use a Jacobian-transpose-based force control algorithm to emulate the abstract model on the articulated leg. Formally this is:

$$\tau = J_{leg}^T F_v, \quad (1)$$

where F_v is the force that the virtual spring-damper model produces, J_{leg}^T is the leg Jacobian transpose and τ is the torque vector that the relevant joint actuators are called to produce.

This allows us to experiment with various spring and damper parametrizations without changing the physical characteristics of the robot. We can change the stiffness of the virtual spring, the damping coefficient and the resting length of the virtual model on-the-fly. It allows for controlled compliance for the legs, something crucial for absorbing impact forces generated by the feet touchdown, for disturbance rejection, and for equalizing the support forces exerted by the support legs. Note that hydraulic actuation is inherently very stiff.

B. Trotting controller

For trotting with HyQ we set a clear preferred direction of motion in the sagittal plane. This way the trotting controller considers the dynamics of the sagittal and the coronal planes separately whilst utilising similar feedback-based control loops. In brief we track a desired velocity in the sagittal plane and dissipate disturbances in the coronal plane.

In addition, trotting naturally separates the four legs into two diagonal pairs that alternate between swing and support phases. The support legs need to make attitude corrections, equalize the force between the supporting pair and to produce a vertical thrusting force. The swing legs on the other hand are retracted for most of the swing phase and are lengthened before touching down. The swing legs are positioned for touchdown according to a metric derived from the *stance phase symmetry* assumption, that explicitly depends on the robot's velocity, as explained below in V-B.1.

TABLE I
CONTROLLER PARAMETRIZATION USED FOR ALL TESTS IN SIMULATION AND ON THE REAL ROBOT.

Parameter	Value
Spring stiffness	5 kN/m per leg
Damping coefficient	125 Ns/m
Support rest length	0.60 m
Swing rest length	0.50 m
Apex height	0.58 m
Velocity range	0 – 1.0 m/s

All the different tasks that the controller performs are organised into a state machine [2]. The state progression is event driven, which on one hand simplifies the parametrization and bookkeeping of the controller, but on the other hand allows only indirect control of the timing of the different phases of the gait. Fig. 3 provides a sketch of the state machine implementation. Note that both phases occur simultaneously and the leg pairs are switched at every gait cycle. Below we provide a detailed description on the key tasks of the controller.

1) *Positioning for landing*: The position for landing task controls where the swing legs land. It is a control loop that is crucial for the stability of the system. This task utilizes feedback from the on-board *inertial measurement unit* (IMU) about the velocity and the attitude of the system, and the set desired velocity to calculate the hip angle of the virtual telescopic leg. Formally this procedure amounts to calculating the *velocity neutral* landing position and thus the appropriate virtual hip angle:

$$\theta_n = \sin^{-1} \left(\frac{v_x T_s}{2\ell_0} \right), \quad (2)$$

where v_x is the robot forward velocity in the sagittal plane, T_s is an estimate of the stance phase duration and ℓ_0 is the rest length of the virtual spring-damper model (similar to [2]). After this, a simple servo on the error from the desired velocity is utilized to offset the landing point forward or backward, so as to decelerate or accelerate the system, following the SLIP model symmetry assumption. Formally this is:

$$\theta_{des} = \theta_n - k_v (v_{des} - v_x), \quad (3)$$

where θ_{des} is the desired virtual leg hip angle, v_{des} is the desired velocity in the sagittal plane and k_v is a gain for the velocity correction. The same feedback loop is implemented for the coronal plane with the difference that the desired lateral velocity is set to zero and the correction gain being accordingly higher. Both resulting virtual hip angles are also corrected according to the attitude of the robot.

2) *Force equalization*: The impact force-peak of the feet touchdown is absorbed by the actively-compliant behaviour of the legs. Note that there is no guarantee that the legs land simultaneously, this way our active compliance scheme plays a crucial role in absorbing the landing force-peaks. After this we need to equalize the forces that the support legs exert to

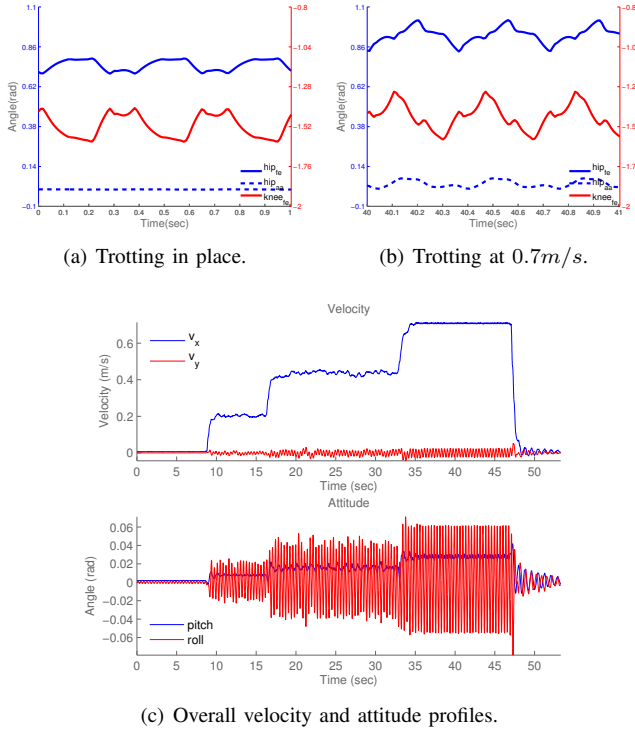


Fig. 4. (a) A one second sequence that shows the motion of the left front leg DoFs while the robot is trotting in place. (b) A one second sequence that shows again the same DoFs while the robot is trotting with a constant forward velocity of 0.7m/s. This corresponds to the later part of the velocity plot that follows in (c). Also note how the amplitude of the motion has grown and the increased need for lateral corrections as depicted by the hip abduction-adduction joint. (c) Plots of the velocity and attitude of the robot throughout this simulation run. Note that the pitch and roll oscillations do not exceed 0.06rad.

the robot body so that undesired moments are removed. We achieve this by measuring the length of the virtual spring elements and accordingly setting their rest lengths (ℓ_0), much like a virtual force differential.

3) *Thrust control*: Thrusting occurs when the virtual springs are fully compressed. The vertical thrust force is calculated in the robot’s coordinate frame and it is parallel to the vertical axis. This is the force vector that will be generated by the support legs and is transformed to the equivalent torque vectors with a transpose Jacobian projection. The magnitude of the force is computed by comparing the desired trotting apex height with the trotting height estimate of the previous gait cycle and accordingly adjusting as:

$$F_v = \frac{h_{des}}{h_{est}} K_h F_{v'}, \quad (4)$$

where F_v is the vertical thrust force magnitude of both support legs, h_{des} is the desired apex height, h_{est} is the previous apex height estimate, K_h is a gain regulating how aggressive the correction should be and $F_{v'}$ is the force magnitude of the previous cycle.

Manipulating the desired trotting apex height can produce gaits with large flight phase or very small flight phase. In practice the latter is preferred as large hops require large torques on the knees and hips. On the real robot we set the

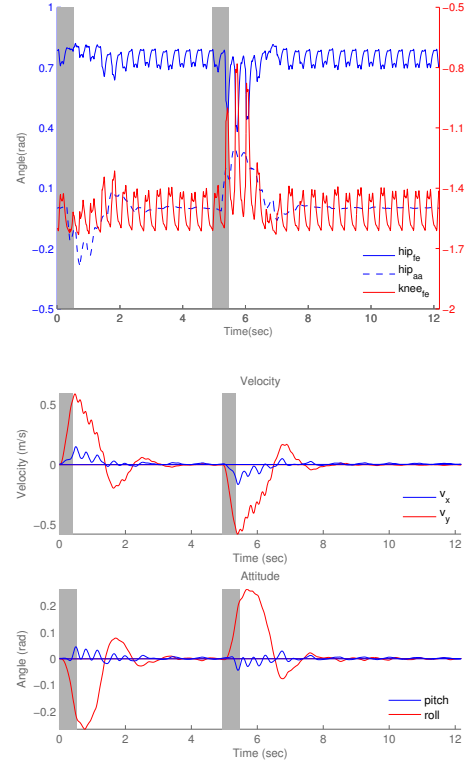


Fig. 5. Two pushes that push the robot’s body laterally for more than 0.5m. These two unexpected perturbations are of opposite direction and a magnitude of 500N while they act for 0.5s. The gray shaded areas represent the duration of the lateral force. *Top*: The left front DoFs while the robot recovers from this unexpected perturbation. *Bottom*: The attitude and velocity profiles of the robot body. Corresponding snapshots are available in Fig. 7.

desired trot apex to a height that fully extends the virtual spring elements, thus leading to a very short flight phase.

4) *Attitude control*: Corrections to the body attitude are performed by the support leg pair before thrusting. This happens when the support legs are loaded with the body weight and follow a simple feedback loop. The angle of the virtual telescopic leg is calculated with respect to the attitude of the quadruped. This is done by combining the absolute orientation of the robot body (IMU quaternion orientation) and the current state of the leg joints (proprioception).

5) *Extension and retraction*: We control the extension and the retraction of the legs by manipulating the resting lengths of the virtual spring element of each articulated leg. To avoid step changes we use a 5th order spline to transition from short to long virtual spring rest lengths and vice-versa.

VI. RESULTS

We conducted experiments both in simulation and on the real robot. For the tests in simulation we used the physics based simulator *SL* [18], that utilizes a detailed rigid body model of the robot dynamics. We demonstrate successful trotting in simulation and on the real system with the same controller and the same set of parameters, while we also show how the system responds to large unexpected disturbances in simulation.

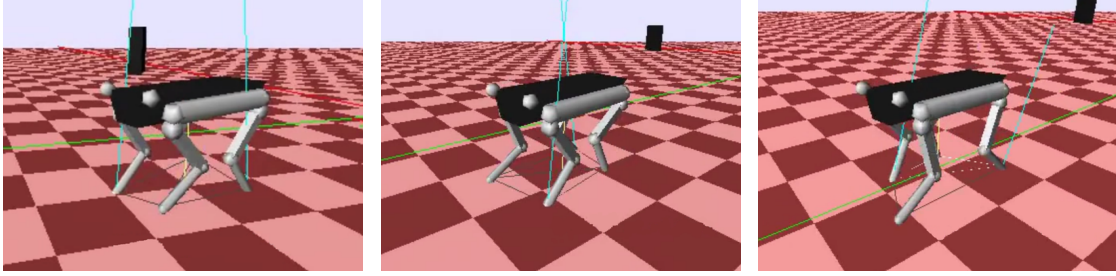


Fig. 6. Snapshots from the accompanying video showing the robot trotting in simulation. From left to right, trotting at a speed of $0.5m/s$, at $1.0m/s$ and $1.5m/s$. Note that currently we do not compensate for any disturbances in yaw, this way the orientation of the robot can change. Link to video available at the Appendix.

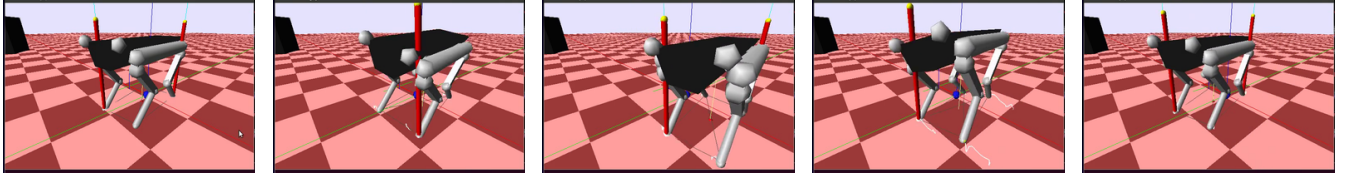


Fig. 7. Snapshots showing the robot being pushed laterally in simulation. These snapshots follow the data available in Fig. 5. From left to right: the robot trotting in place and a lateral force of $500N$ has been applied for $0.5s$. The robot is pushed sideways by this force for over $0.5m$, dissipates the perturbation and continues trotting stably in place. Another force of the same magnitude and duration is applied with the opposite direction and the robot successfully recovers. The red bars represent the ground reaction forces and are not physical objects, but help visualise which leg pair is at what phase. Link to video available at the Appendix.

For the implementation of the trotting controller the definition of a number of parameters is required. Related work in biological studies [4], [5], as mentioned earlier, has helped inform such parameter choices, e.g., the length ($\sim 0.6m$) of the virtual spring elements, their extension/retraction displacement ($\sim 0.1m$) and stiffness ($\sim 5kN/m$), the frequency of the stride ($\sim 1.93sec^{-1}$) etc. In our implementation we have followed such parametrization closely.

We have experimented with a range of parametrizations to reach a robust trotting behaviour. Overall, stiffness values below $3.5kN/m$ result in controllers that barely trot as the legs behave very compliantly. In contrast stiffness values above $6.5kN/m$ result in the legs behaving very aggressively, having torque outputs that reach the actuator limits of the real robot. The damping of these elements was experimentally set.

A. Trotting in simulation

Our initial implementation and testing cycle has been performed in simulation. There we were able to test and tune a number of different controller parameter sets and experimentally evaluate their robustness. This culminated in a parameter set that comes very close to what biological observations suggest (Table I).

The trotting controller is capable of trotting in place where it maintains the body attitude very close to zero, while it gently hops up to an apex height just longer than the virtual spring elements. Note that we aim at trot-walking as trot-running requires knee and hip torques that are close to the limits on real robot. We ramp up the desired forward velocity of the robot in three discrete steps and the robot responds with an analogous increase of its forward trotting velocity. In Fig. 4 we present a run of this procedure. The plots (a) and

(b) show the evolution of the robots' front left leg degrees of freedom while in (a) it trots in place, and while in (b) the robot is trotting with a forward velocity of $0.7m/s$. Fig. 4 (c) presents the robot velocity and attitude throughout this simulation trial.

We note that while the robot trots in place the disturbance to its attitude is very small, as the velocity increases we observe an amplification in the coronal plane swing while a nose down pitching motion is also observed. We attribute this effect to the elbow-backward/knee-forward configuration of the system that has been shown to produce passively a nose-down pitching moment [19]. With regards to individual leg DoFs (Fig. 4(a) and (b)) we see that the amplitude of the motion of each joint scales with the velocity. The effect is more underlined with regards to the hip abduction-adduction joint (hip_{aa}) which makes little to no corrections when trotting in place but plays a crucial role for the robot stability as the velocity increases. Example snapshots of the

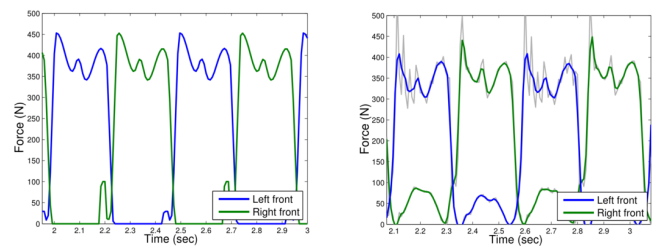


Fig. 8. Ground reaction forces when trotting in simulation (*left*) and on the real robot (*right*). On the real robot the GRF signals are passed through a low-pass filter while the grey line shows the unfiltered signal.

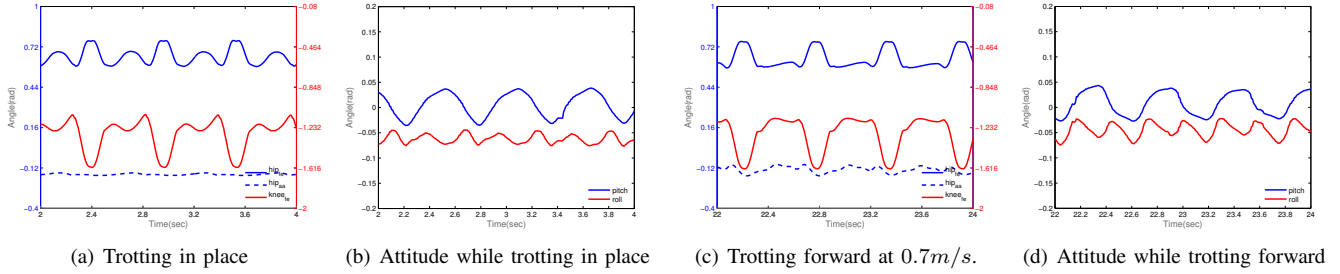


Fig. 9. Trotting experiments on the real robot. (a) A two second sequence showing the motion of the left front leg DoFs while the robot is trotting in place. (b) The attitude of the robot while trotting in place, corresponding to the data sequence presented in (a). (c) A two second sequence that showing again the same DoFs while the robot is trotting with a constant forward velocity of $0.7m/s$. (d) The attitude of the robot while trotting forward, corresponding to the data sequence presented in (c). Note that in both cases the pitch and the roll of the robot oscillate with an amplitude that is less than $0.1rad$. The roll of the robot is always offset from 0.0 as a result of the external oil supply hoses that apply a constant (unmodelled) external force to the robot.

robot trotting in simulation are available in Fig. 6 while Fig. 8(left) shows the ground reaction forces (GRFs) of two trotting cycles.

B. Push recovery

A showcase of the controller robustness is the ability to recover from unexpected perturbations. Due to the morphology of the robot, perturbations along the coronal plane are much harder to accommodate. We have tested the response of the controller while trotting in place and while trotting at a constant velocity.

We exert unexpected forces on the robot body that are up to $500N$ in magnitude and are applied for up to $0.5s$. Such a perturbation pushes the robot's body more than $0.5m$. When trotting in place and when trotting in the specified velocity range the robot can successfully recover from perturbations that fall under the aforementioned specifications. Fig. 5 shows how the controller responds to forces of $500N$ and duration of $0.5s$. The grey shaded time margins represent the duration of the force application, the first force being along the positive and the second along the negative direction of the coronal plane (y axis). These forces are applied at the center of the robot's body.

Fig. 5 (top) shows how the left forward leg DoFs respond to dissipate the perturbations. Fig. 5 (bottom) presents the attitude and the velocity of the robot body as it is pushed laterally by the unexpected force, and how the disturbances are dissipated. Snapshots from this test are presented in Fig. 7.

C. Trotting with the robot

We tested our trotting controller on the real quadruped robot with similar success. We have used the same controller parametrization as in simulation, and we experimented with the robot trotting in place, trotting forward and backward. We begin with the robot standing in place while the state machine is activated by setting the leg extension/retraction offset to zero. We then gradually increase the leg offset, that leads first to a gentle rocking motion and then to the legs lifting off the ground. The desired forward/backward velocity can then be manipulated accordingly.

Fig. 9 shows the left front leg DoFs, velocity and the attitude profiles of the robot trials. Fig. 9 (a) and (b) present the relevant DoFs while the robot is trotting in place (also Fig. 10) and Fig. (c) and (d) present the same DoFs while the robot is trotting forward at a speed of $\sim 0.7m/s$. The attitude signals in both scenarios have been filtered with a low-pass filter. Fig. 8 (right) shows the (GRFs) of two trotting cycles. Fig. 10 and 11 present snapshots from equivalent video sequences of HyQ trotting in place, trotting forward and trotting backward. The complete video sequences are available as accompanying material following the link at the Appendix.

Overall, the transition from simulation to the real robot has been smooth. Our experience on the real platform has been similar to the simulation, something that we attribute to the use of the same controller code and to the detailed model of the robot's mechanical parameters (e.g. leg segment inertia matrices). This was only possible because our robot is designed and built *in-house*, thus leading to a very realistic dynamics model.

A number of other considerations with regards to the lower level control of the actuators, the utilized torque controllers and issues with such low-level loops are beyond the scope of this paper but have been addressed in [16].

VII. CONCLUSION

We presented a trotting controller for a robotic quadruped, that utilises a virtual spring and damper abstraction for producing actively compliant behaviour, crucial for the smooth interaction of such a sizeable robot with its environment. We showed how the controller is organised and how the different tasks are implemented. Controllers based on such simple feedback loops have been shown to work with very compliant telescopic legs in the past. To our knowledge, we are the first to report results of such controllers on a fully actuated quadruped with articulated legs and no physical compliant elements. We presented how this trotting controller is able to trot at varying speeds in simulation how it can robustly dissipate unexpected perturbations of sizeable magnitude and duration. We presented results in simulation and tested our approach, unaltered, with the real quadruped robot. We have



Fig. 10. Snapshots of a video of the HyQ robot trotting in place. From left to right: the swing legs are shortening while the support legs are supporting the robot's weight and correcting the posture. Two snapshots later the swing pair lands, the leg pairs switch and the state machine cycle continues. In the background the off-board oil pump that has been used throughout our experiments is visible. Link to video available at the Appendix.



Fig. 11. Snapshots of a video of the HyQ robot trotting forward with a forward velocity of $\sim 0.7m/s$. The data presented in Fig. 9 correspond to a two second time interval extracted from this trotting sequence. Link to video available at the Appendix.

shown how a dynamic, feedback-based controller that has been experimentally optimised in simulation can successfully transfer to the real quadruped robot.

As for future work, we are currently developing a scheme that scales the stiffness of the support legs as well as the foot clearance distance of the swing legs in proportion to the forward and lateral velocities of the robot. As mentioned before we are also working on a more elaborate method for the state estimation of the quadruped, crucial for the success of highly dynamic control. In addition we began experimenting with exponential models of virtual spring elements. Such model might add in complexity to the controller but can provide significant benefits. Namely, we aim to achieve very compliant behaviour during leg touchdown that stiffens-up exponentially as the virtual spring is compressed, this way providing a more firm support the more load the leg accepts. Last but not least, we are preparing our robot for field testing, which will give us the opportunity to experiment with more dynamic behaviour in a natural environment.

APPENDIX

The accompanying video can be accessed at the following link, <http://youtu.be/K0LwO4GKMnE?hd=1>.

ACKNOWLEDGEMENTS

The authors would also like to thank Marco Frigerio, Thiago Boaventura, Michele Focchi, Hamza Khan, Stephane Bazeille, Jake Goldsmith and our team of technicians. This research is funded by the Fondazione Istituto Italiano di Tecnologia.

REFERENCES

- [1] C. Semini, N. G. Tsagarakis, E. Guglielmino, M. Focchi, F. Cannella, and D. G. Caldwell, "Design of HyQ – a hydraulically and electrically actuated quadruped robot," *Proceedings of the Institution of Mechanical Engineers, Part I: Journal of Systems and Control Engineering*, vol. 225, no. 6, pp. 831–849, 2011.
- [2] M. H. Raibert, *Legged robots that balance*. Cambridge, MA, USA: The MIT Press, 1986.
- [3] T. McMahon and G. Cheng, "The mechanics of running: How does stiffness couple with speed?" *Journal of Biomechanics*, vol. 23, no. SUPPL. 1, pp. 65–78, 1990, cited By (since 1996) 286.
- [4] N. C. Heglund and C. R. Taylor, "Speed, stride frequency and energy cost per stride: how do they change with body size and gait?" *Journal of Experimental Biology*, vol. 138, no. 1, pp. 301–318, 1988.
- [5] C. T. Farley, J. Glasheen, and T. A. McMahon, "Running springs: speed and animal size," *Journal of Experimental Biology*, vol. 185, no. 1, pp. 71–86, 1993.
- [6] D. V. Lee and A. A. Biewener, "Bigdog-inspired studies in the locomotion of goats and dogs," *Integrative and Comparative Biology*, vol. 51, no. 1, pp. 190–202, 2011.
- [7] I. Poulakakis, E. Papadopoulos, and M. Buehler, "On the stability of the passive dynamics of quadrupedal running with a bounding gait," *The International Journal of Robotics Research*, vol. 25, 2006.
- [8] J. Estremera and K. J. Waldron, "Thrust control, stabilization and energetics of a quadruped running robot," *Int. J. Rob. Res.*, vol. 27, pp. 1135–1151, October 2008.
- [9] G. Hawker and M. Buehler, "Quadruped trotting with passive knees: design, control, and experiments," in *2000 IEEE International Conference on Robotics and Automation (ICRA'00)*, vol. 3, 2000.
- [10] Y. Yamada, S. Nishikawa, K. Shida, R. Niiyama, and Y. Kuniyoshi, "Neural-body coupling for emergent locomotion: a musculoskeletal quadruped robot with spinobulbar model," in *2011 IEEE/RSJ International Conference on Intelligent Robots and Systems (IROS2011)*, San Francisco, CA, USA, September 2011, pp. 1499–1506.
- [11] K. Kotaka, B. Ugurlu, M. Kawanishi, and T. Narikiyo, "Prototype development and real-time trot-running implementation of a quadruped robot: Robocat-1," in *2013 IEEE International Conference on Mechatronics (ICM13)*, February 2013.
- [12] M. Hildebrand, "The Quadrupedal Gaits of Vertebrates," *BioScience*, vol. 39, no. 11, 1989.
- [13] N. C. Heglund, C. R. Taylor, and T. A. McMahon, "Scaling stride frequency and gait to animal size: Mice to horses," *Science*, vol. 186, no. 4169, pp. 1112–1113, 1974.
- [14] R. M. Alexander, "Models and the scaling of energy costs for locomotion," *Journal of Experimental Biology*, vol. 208, no. 9, pp. 1645–1652, 2005.
- [15] C. Semini, "HyQ - design and development of a hydraulically actuated quadruped robot," Ph.D. dissertation, Italian Institute of Technology and University of Genoa, 2010.
- [16] T. Boaventura, C. Semini, J. Buchli, M. Frigerio, M. Focchi, and D. G. Caldwell, "Dynamic torque control of a hydraulic quadruped robot," *Robotics and Automation (ICRA), 2012. IEEE International Conference on*, 2012.
- [17] M. Focchi, T. Boaventura, C. Semini, M. Frigerio, J. Buchli, and D. G. Caldwell, "Torque-control based compliant actuation of a quadruped robot," in *Proc. of the 12th IEEE Int. Workshop on Advanced Motion Control (AMC)*, 2012.
- [18] S. Schaal, "The SL simulation and real-time control software package," Tech. Rep., 2009.
- [19] D. V. Lee and S. G. Meek, "Directionally compliant legs influence the intrinsic pitch behaviour of a trotting quadruped," *Proceedings of the Royal Society B: Biological Sciences*, vol. 272, no. 1563, pp. 567–572, 2005.